The Origin of Outflows in Evolved Stars
Proceedings IAU Symposium No. 366, 2022
L. Decin, A. Zijlstra & C. Gielen, eds.
doi:10.1017/S1743921322000497

Shaping the initial-final mass relation of white dwarfs with AGB outflows

Paola Marigo

Department of Physics and Astronomy G. Galilei, University of Padova,
Vicolo dell'Osservatorio 3,i IT-35136, Padova, Italy
email: paola.marigo@unipd.it

Abstract. A recent analysis of a few carbon-oxygen white dwarfs in old open clusters of the Milky Way (MW) identified a kink in the initial-final mass relation (IFMR), located over a range of initial masses, $1.65 \lesssim M_{\rm i}/M_{\odot} \lesssim 2.10$, which unexpectedly interrupts the commonly assumed monotonic trend. The proposed interpretation links this observational fact to the formation of carbon stars and the modest outflows (with mass loss rate $< 10^{-7}\, M_{\odot}/{\rm yr}$) that are expected as long as the carbon excess remains too low to produce dust grains in sufficient amount. Under these conditions the mass of the carbon-oxygen core can grow more than is generally predicted by stellar models. We discuss these new findings also in light of a new systematic follow-up investigation, based on Gaia EDR3, of evolved giants (13 carbon stars, 3 S stars and 4 M stars) belonging to intermediate-age open clusters.

Keywords. stars: evolution, stars: AGB and post-AGB, stars: mass loss, stars: winds, outflows, stars: white dwarfs, stars: abundances, stars: atmospheres

1. Introduction

The IFMR connects the mass of a star on the main sequence, $M_{\rm i}$, with the mass, $M_{\rm f}$, of the WD left at the end of its evolution. This fate (Herwig 2005) is common to low- and intermediate-mass stars ($0.9 \lesssim M_{\rm i}/M_{\odot} \lesssim 6-7$) that, after the exhaustion of helium in the core, experience the AGB phase and produce carbon-oxygen WDs. Quasi-massive stars ($8 \lesssim M_{\rm i}/M_{\odot} \lesssim 10$) that, after the carbon burning phase evolve through the Super-AGB phase, may also produce oxygen-neon-magnesium WDs. In both evolutionary scenarios stellar winds play a key role in determining the final mass of the compact remnant.

To derive the semi-empirical IFMR, singly-evolved WDs that are members of star clusters are ideally used (Cummings et al. 2018). Spectroscopic analysis provides their atmospheric parameters, that is, surface gravity, effective temperature, and chemical composition. Coupling this information to appropriate WD cooling models provides the WD mass, its cooling age, and additional parameters for testing cluster membership and single-star status. Finally, subtracting a WD's cooling age from its cluster's age gives the evolutionary lifetime of its progenitor, and hence its $M_{\rm i}$.

2. The detection of IFMR kink

A recent work (Marigo et al. 2020) identified a kink in the IFMR at $M_{\rm i} \simeq 2\, M_{\odot}$, following updated analyses of a few WDs members of intermediate-age open clusters (NGC 7789, NGC 752, Ruprecht 147, with ages $\simeq 1.5-2.5$ Gyr). The new results were obtained with a novel analysis technique that combines photometric and spectroscopic data to better constrain the WD parameters. The data are shown in Fig. 1 (diamonds with error bars). While the steep increase in the IFMR near $M_{\rm i} \simeq 1.65\, M_{\odot}$ is at present well

https://doi.org/10.1017/S1743921322000497 Published online by Cambridge University Press

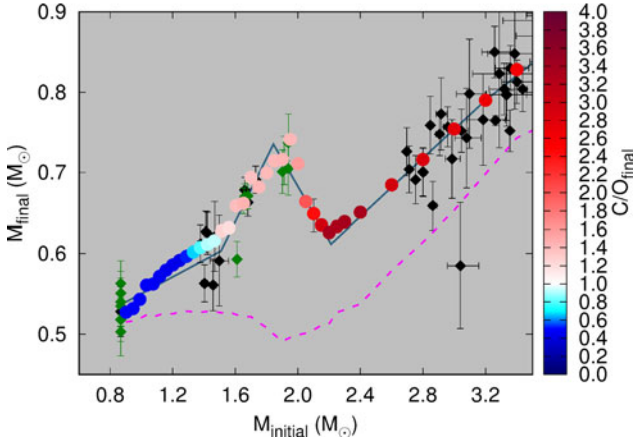

Figure 1. The semi-empirical IFMR (diamonds with errors bars) from Cummings et al. (2018) and Marigo et al. (2020), with the 7 newly discovered and 12 newly analysed WDs shown in green. Error bars cover a range of $\pm 1\,\sigma$. Superimposed is the theoretical IFMR obtained with state-of-the art mass-loss prescriptions for mass loss in carbon stars, in combination with calibrated efficiency λ of the third dredge-up, color-coded as a function of the final C/O at the end of the TP-AGB phase (right color bar). The theoretical core mass at the first thermal pulse is also shown (magenta dashed line).

constrained, further data are needed to better probe the decreasing IFMR for $M_{\rm i} \gtrsim 2\, M_\odot$. However, we underline that after this rapid rise such a temporary decrease is necessary to keep consistency with the observed field-WD mass distribution. For example, if this steep rise was instead followed by a plateau at $M_{\rm f} \sim 0.7\, M_\odot$, then every progenitor with $1.9 \lesssim M_{\rm i}/M_\odot \lesssim 2.8$ would create a $\sim 0.7\, M_\odot$ WD, substantially overproducing field WDs at this mass compared with observations.

3. The physical interpretation of the IFMR: the role of AGB winds

We interpret the kink in the IFMR as the signature of the lowest-mass stars in the MW that became carbon stars during the TP-AGB phase. The proposed explanation is as follows. At solar-like metallicity low-mass carbon stars ($1.65 \lesssim M_{\rm i}/M_\odot \lesssim 1.90$) attain low C/O ratios ($\lesssim 1.3$) and low values of the excess of carbon compared to oxygen, C − O, in the atmosphere. The quantity C − O is particularly relevant as it measures the budget of free carbon, not locked in the CO molecule, available to condense into dust grains. In fact, state-of-the-art dynamical models for carbon stars (Bladh et al. 2019; Eriksson et al. 2014; Mattsson et al. 2010) predict that a minimum carbon excess, $({\rm C-O})_{\rm min}$, is necessary to generate dust-driven winds, with mass-loss rates exceeding a few $10^{-7}\, M_\odot\, {\rm yr}^{-1}$. We recall that according to a standard notation, ${\rm C-O} = \log(n_{\rm C} - n_{\rm O}) - \log(n_{\rm H}) + 12$, where $n_{\rm C}$, $n_{\rm O}$, and $n_{\rm H}$ denote the number densities of carbon, oxygen, and hydrogen, respectively.

The existence of a threshold in carbon excess impacts on the TP-AGB evolution and hence on the IFMR. In TP-AGB stars the surface enrichment of carbon is controlled by the 3DU, a series of mixing episodes that happen each time the base of the convective envelope is able to penetrate into the inter-shell region left at the quenching of a thermal pulse. The efficiency of a 3DU event is commonly described by the dimensionless parameter $\lambda = \Delta M_{\rm 3DU}/\Delta M_{\rm c}$, defined as the amount of dredged-up material, $\Delta M_{\rm 3DU}$, relative to the growth of the core mass, $\Delta M_{\rm c}$, during the previous inter-pulse period.

Figure 2 illustrates how the efficiency of 3DU regulates the increase of the surface C/O and hence the carbon excess; how the latter, in turn, affects the mass-loss rate, hence the lifetime of a carbon star and eventually the final mass of the WD. The models refer

https://doi.org/10.1017/S1743921322000497 Published online by Cambridge University Press

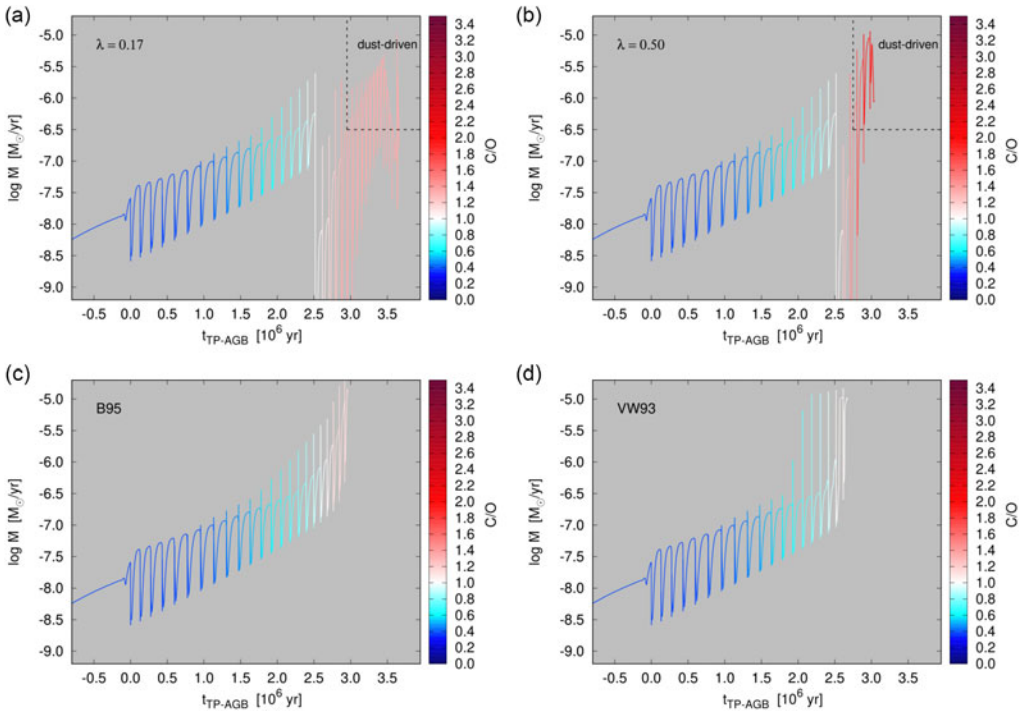

Figure 2. Evolution of the mass-loss rate during the whole TP-AGB evolution of a star with $M_{\rm i} = 1.8\,M_{\odot}$ and solar metallicity. Time is set to zero at the first TP. The tracks are colour-coded according to the current photospheric C/O ratio. Calculations differ in the treatment of mass loss and/or in the efficiency λ of the 3DU. **a** - **b**, Models in which mass loss during the carbon star phase does depend on the carbon excess (Mattsson et al. 2010; Bladh et al. 2019). The 3DU is less efficient in model **a** compared to model **b**. Inside the region delimited by the dotted lines stellar winds are driven by carbonaceous dust grains. **c** - **d**, Results obtained with widely-used mass-loss formalisms (Bloecker 1995) that, unlike in **a** and **b**, do not contain an explicit dependence on the carbon abundance.

to a star with $M_{mi} = 1.8\,M_{\odot}$ and $Z = 0.014$, near the kink's peak of the semi-empirical IFMR. The two cases in Fig. 2 share the same set of input prescriptions, except that the 3DU is shallow in the model **a** ($\lambda \simeq 0.17$), and much more efficient in the model **b** ($\lambda = 0.5$ as the star becomes C-rich). In both cases, as soon as the star reaches $\mathrm{C/O} > 1$, a sudden drop in the mass-loss rate is expected to occur. This prediction deserves to be explained in detail. The transition from $\mathrm{C/O} < 1$ to $\mathrm{C/O} > 1$ marks a radical change both in the molecular abundance pattern of the atmosphere (shifting from O-bearing to C-bearing species; see Marigo & Aringer 2009), and in the mineralogy of the dust that could in principle condense in the coolest layers.

When a carbon star is born, the silicate-type dust that characterises the circumstellar envelopes of M-type stars is no longer produced and the composition of the grains that may actually form suddenly changes, switching mainly to silicon carbide and amorphous carbon (Ferrarotti & Gail 2006). The key point is that the growth of carbonaceous dust requires suitable physical conditions (e.g., temperature, density and chemical composition of the gas, stellar radiation field), and these may not always be fulfilled as soon as $\mathrm{C/O} \gtrsim 1$. In addition, carbonaceous grains are expected to drive a wind only if they form in sufficient amount (Mattsson et al. 2010; Bladh et al. 2019), a condition expressed by the threshold $(\mathrm{C}-\mathrm{O})_{\rm min}$. It follows that, as long as the atmospheric abundance of

https://doi.org/10.1017/S1743921322000497 Published online by Cambridge University Press

free carbon is small, typically during the early carbon-star stages, dust grains cannot be abundantly produced.

The natural conclusion is that if carbonaceous dust grains are not abundant enough to drive a powerful wind, when C/O just exceeds unity, then only a modest outflow may be generated, possibly sustained by small-amplitude pulsations, like those of Semi-regular variable stars (McDonald & Trabucchi 2019). These conditions apply to the model **a** of Fig. 2, which experiences a shallow 3DU. The C/O ratio grows slowly (maximum of $\simeq 1.33$), the star stays in a phase of very low mass loss until the threshold in carbon excess is slightly overcome and a moderate dust-driven wind is eventually activated, with mass-loss rates not exceeding few $10^{-6}\, M_{\odot}\ \mathrm{yr}^{-1}$. Also the model **b** enters a phase of low mass loss soon after the transition to carbon star, but then its evolution proceeds differently. As the 3DU is more efficient, C/O increases more rapidly (maximum of $\simeq 1.91$), so that the threshold in carbon excess is largely overcome, a powerful dust-driven wind is generated, and the mass-loss rate rises up to $\simeq 10^{-5}\, M_{\odot}\ \mathrm{yr}^{-1}$.

These model differences affect the carbon star lifetimes and, in turn, the final masses left after the TP-AGB phase. In the model **a** the carbon star phase lasts $\simeq 1.15$ Myr and produces a WD with a final mass of $\simeq 0.732\, M_{\odot}$. In the model **b** the duration of the carbon star phase is halved, $\simeq 0.52$ Myr, and terminates with a WD mass of $\simeq 0.635\, M_{\odot}$. Likewise, shorter lifetimes and lower final masses are obtained if we adopt mass-loss formulations that do not depend on the carbon abundance. In Fig. 2 we also show two examples (panels **c, d**) in which we use the Bloecker (1995) and Vassiliadis & Wood (1993) relations. Both predict a systematic increase of the average mass-loss rate as the star evolves on the TP-AGB. The resulting WD masses are $0.646\, M_{\odot}$ and $0.615\, M_{\odot}$, respectively.

4. Calibration of the 3DU efficiency

The analysis presented above indicates that the final WD masses of the progenitor carbon stars are the result of the interplay between mass loss and third dredge-up. In light of this, we computed a large grid of TP-AGB models with `COLIBRI` (Marigo et al. 2013) that cover a relevant region of the parameter space $(M_{\mathrm{i}}, \lambda)$, assuming solar initial metallicity. M_{f} of carbon stars anticorrelates with λ. At this point, the natural step is to pick up the $(M_{\mathrm{i}}, \lambda)$ combinations that best approximate the semi-empirical IFMR. The detected IFMR kink over the range $1.65 \lesssim M_{\mathrm{i}}/M_{\odot} \lesssim 2.0$ is well recovered by assuming that these stars experience a shallow 3DU during the TP-AGB phase, typically with $0.1 \lesssim \lambda \lesssim 0.2$. In this regard, we note that observations of TP-AGB stars in Galactic open clusters (see Sect. 5) indicate that carbon stars slightly less massive than $\simeq 1.65\, M_{\odot}$ can be formed at solar metallicity, with an initial mass $M_{\mathrm{i}} \simeq 1.5\, M_{\odot}$. At this M_{i} the semi-empirical IFMR show white dwarfs with $M_{\mathrm{f}} \lesssim 0.62\, M_{\odot}$, therefore without clear evidence of an excess of mass, unlike at higher M_{i}. From a theoretical point of view this is easily explained by assuming that the transition to C-rich phase occurred quite late during the TP-AGB evolution, when a substantial fraction of the envelope had already been expelled by the O-rich winds. Under these conditions, the growth of the core mass could not proceed significantly. Overall, stars with $1.5 \lesssim M_{\mathrm{i}}/M_{\odot} < 1.8$ are those just massive enough to become carbon stars. They are little enriched in carbon, with low final ratios ($1.1 \lesssim \mathrm{C/O} \lesssim 1.4$) and low carbon excesses. At larger masses the 3DU becomes more efficient and powerful dust-driven winds are activated. The results of our calibration are shown in Fig. 1.

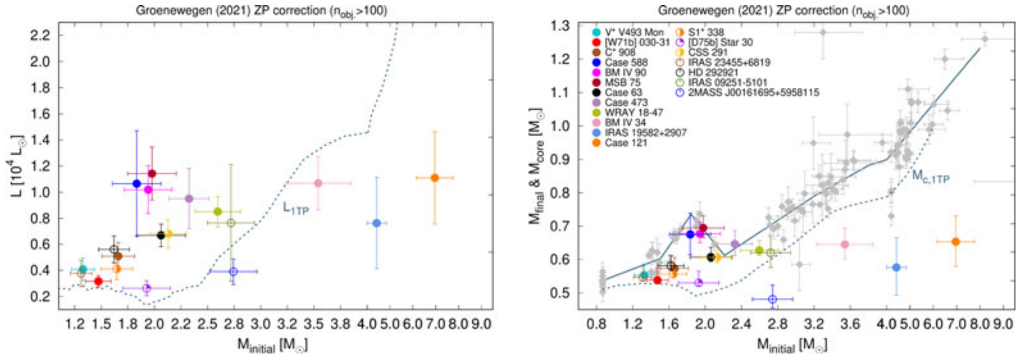

Figure 3. Luminosities and core masses of TP-AGB stars in open clusters as a function of the initial stellar mass. The M, S, and C stars (reported in the legend) are marked with colored symbols and error bars. For comparison we over-plot the luminosity and core mass at the first thermal pulse, L_{1TP} and $M_{c,1TP}$, predicted by the PARSEC stellar models (Bressan et al. 2012) at solar metallicity (dashed line). The cluster ages and visual extinctions are taken from the work of Cantat-Gaudin et al. (2020). Gaia EDR3 parallaxes are corrected for the zero-point offset following Groenewegen (2021). Note that the X-axis is stretched over the range $0.8 \leq M_i/M_\odot \leq 4.0$. *Left panels*: Bolometric luminosties derived from the fitting of the spectral energy distributions. *Right panels*: The initial-final mass relation of white dwarfs in the Milky Way is compared to the current core masses of TP-AGB stars in open clusters. The semi-empirical IFMR (gray diamonds with error bars) is taken from Marigo et al. (2020) and Cummings et al. (2018). The solid line is a fit to the IFMR data.

5. AGB stars in Galactic open clusters

Benefiting from the *Gaia* DR2 and EDR3 releases of photometric and astrometric data we examine the population of asymptotic giant branch stars that appear in the fields of intermediate-age and young open star clusters (Marigo et al. (2022)). We identify 49 AGB star candidates, brighter than the tip of the red giant branch, with a good-to-high cluster membership probability. Among them we find 19 TP-AGB stars with known spectral type: 4 M stars, 3 MS/S stars and 12 C stars. By combining observations, stellar models, and radiative transfer calculations that include the effect of circumstellar dust, we characterize each star in terms of initial mass, luminosity, mass-loss rate, core mass, period and mode of pulsation (see Fig. 3). The information collected helps us shed light on the TP-AGB evolution at solar-like metallicity, placing constraints on the third dredge-up process, the initial masses of carbon stars, stellar winds, and the initial-final mass relation (IFMR). In particular, we find that two bright carbon stars, MSB 75 and BM IV 90, members of the clusters NGC 7789 and NGC 2660 (with similar ages of $\simeq 1.2 - 1.6$ Gyr and initial masses $2.1 \gtrsim M_i/M_\odot \gtrsim 1.9$), have unusually high core masses, $M_c \approx 0.67 - 0.7\, M_\odot$. These results support the detection of the IFMR kink and its proposed interpretation in terms of carbon-star formation and AGB outflows.

6. Conclusions

A new thorough analysis of a few WDs in old open clusters with turn-off masses over the range from $1.6\, M_\odot \lesssim M_i \lesssim 2.1\, M_\odot$ has revealed that the IFMR exhibits a non-monotonic component, with a peak of $M_f \approx 0.70 - 0.75\, M_\odot$ at $M_i \simeq 1.8 - 2.0\, M_\odot$. It happens just in proximity of the transition mass, $M_i \simeq M_{HeF}$, between low-mass stars that experience the He-flash in their degenerate He-cores at tip of the red giant bracng phase, and intermediate-mass stars that avoid electron degeneracy.

The proposed physical interpretation is that the IFMR kink marks the formation of solar-metallicity low-mass carbon stars. These latter experienced a shallow 3DU

https://doi.org/10.1017/S1743921322000497 Published online by Cambridge University Press

($\lambda \simeq 0.1 - 0.3$) during the TP-AGB phase, so that the amount of carbon dust available to trigger a radiation-driven wind was small and $\dot{M}$ remained mostly below a few $10^{-6}\, M_{\odot}\,\mathrm{yr}^{-1}$. These circumstances led to a prolongation of the TP-AGB phase with the consequence that fairly massive WDs ($M_{\mathrm{f}} > 0.65\, M_{\odot}$), larger than commonly expected, were left at the end of the evolution. The progenitors that populate the IFMR kink are expected to be potentially important contributors to the galaxy emitted light and modest sources of carbon (in the form of gas and dust) at the same time.

In a systematic follow-up study we fully characterized the AGB star population in open clusters, exploiting the new *Gaia* data. Several findings emerge from our study. The minimum initial mass for carbon star formation at solar-like metallicity should not be higher than $\simeq 1.5\, M_{\odot}$, while the maximum mass should not be lower than $3.0 - 4.0\, M_{\odot}$. The 3 stars of type MS and S provide information about the onset of the 3DU and the transition to the C-star domain. The 12 carbon stars are all optically visible, and none appear truly dust-enshrouded. The mass-loss rate for most of them is very low ($\dot{M} \approx 10^{-8}\, M_{\odot}/\mathrm{yr}$), below the typical values that characterize a dust-driven wind, except for two carbon stars of low initial mass (V* V493 Mon and [W71b]).

The photometric variability data we retrieved suggest the stars in the sample are LPVs. The observed periods, in combination with derived absolute magnitudes, are consistent with Mira-like or semi-regular variability. Most of the C-stars appear to be fundamental mode pulsators, while M-, MS- and S-type stars pulsate predominantly in the first overtone mode (consistent with the fact that they are less evolved), except for the S-star S1* 338 whose primary period is attributed to pulsation in the second overtone mode.

The comparison of the estimated M_{c} with the IFMR of the white dwarfs has highlighted a striking fact: the presence of almost dust-free bright carbon stars with $0.65 \lesssim M_{\mathrm{c}}/M_{\odot} \lesssim 0.70$, and initial masses of $\approx 1.9 - 2.0\, M_{\odot}$.

Therefore, our study on AGB stars in open clusters (Marigo et al. (2022)) not only support the existence of the IFMR kink, but also the underlying interpretative hypotheses: the progenitors are 1) carbon stars that 2) experienced modest outflows for a significant fraction of their C-rich phase, 3) with inefficient dust production. In fact, the carbon stars MSB 75 and BM IV 90 ($L \approx 10\,000 - 13\,000\, L_{\odot}$), have an estimated mass-loss rate of $\approx$ few $10^{-8}\, M_{\odot}/\mathrm{yr}$, while their variability is characterized by low-amplitude pulsation. Overall, these new findings are of great significance to constrain the contribution from AGB stars to the chemical enrichment and integrated ligth of galaxies.

References

Bladh, S., Eriksson, K., Marigo, P., et al. 2019, *A&A*, 623, A119
Bloecker, T. 1995, *A&A*, 297, 727
Bressan, A., Marigo, P., Girardi, L., et al. 2012, *MNRAS*, 427, 127
Cantat-Gaudin, T., Anders, F., Castro-Ginard, A., et al. 2020, *A&A*, 640, A1
Cummings, J. D., Kalirai, J. S., Tremblay, P.-E., et al. 2018, *ApJ*, 866, 21
Eriksson, K., Nowotny, W., Höfner, S., et al. 2014, *A&A*, 566, A95
Ferrarotti, A. S. & Gail, H.-P. 2006, *A&A*, 447, 553
Groenewegen, M. A. T. 2021, *A&A*, 654, A20
Herwig, F. 2005, *ARAA*, 43, 435
Lambert, D. L., Gustafsson, B., Eriksson, K., et al. 1986, *ApJS*, 62, 373
McDonald, I. & Trabucchi, M. 2019, *MNRAS*, 484, 4678
Marigo, P., Bossini, D., Trabucchi, M., et al. 2022, *ApJS*, 258, 43
Marigo, P., Cummings, J. D., Curtis, J. L., et al. 2020, *Nature Astron.*, 4, 1102
Marigo, P., Bressan, A., Nanni, A., et al. 2013, *MNRAS*, 434, 488
Marigo, P. & Aringer, B. 2009, *A&A*, 508, 1539
Mattsson, L., Wahlin, R., & Höfner, S. 2010, *A&A*, 509, A14
Schöier, F. L. & Olofsson, H. 2001, *A&A*, 368, 969
Vassiliadis, E. & Wood, P. R. 1993, *ApJ*, 413, 641

https://doi.org/10.1017/S1743921322000497 Published online by Cambridge University Press